

Stereospecific Diphosphination of Activated Acetylenes: A General Route to Backbone-Functionalized, Chelating 1,2-Diphosphinoethenes

Deborah L. Dodds,[†] Mairi F. Haddow,[†] A. Guy Orpen,[†] Paul G. Pringle,^{*,†} and Gary Woodward[§]

School of Chemistry, University of Bristol, Cantock's Close, Bristol BS8 1TS, U.K., and Rhodia Inc., 350 George Patterson Boulevard, Bristol, Pennsylvania 19007

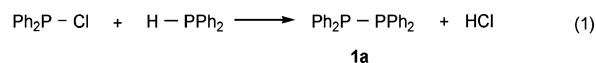
Received August 7, 2006

The symmetrical diphosphanes R_2P-PR_2 {where $R = Ph$ (**1a**), Cy (**1b**), or Bu^t (**1c**)} are made by the reaction of R_2PLi with R_2PCl . The unsymmetrical diphosphanes $R_2P-PR'_2$ {where $R = Bu^t$ and $R' = Ph$ (**2a**); $R = Bu^t$ and $R' = o-Tol$ (**2b**); $R = Cy$ and $R' = Ph$ (**2c**); $R = Cy$ and $R' = o-Tol$ (**2d**); $R = Cy$ and $R' = Bu^t$ (**2e**)} are made by the reaction of $R_2P(BH_3)Li$ with R'_2PCl followed by deprotection with Et_2NH . Diphosphanes **1a,b** and **2a–d** react with $ZC\equiv CZ$ ($Z = CO_2Me$) to give the corresponding $R_2-PCZ=CZPR_2$ (**3a,b**) or $R_2PCZ=CZPR'_2$ (**4a–d**). The reaction of **2a,b** with $HC\equiv CZ$ give the corresponding $R_2PCH=CZPR_2$ (**5a,b**). A mechanism is proposed that accounts for the *cis* stereospecificity and the regioselectivity of these diphosphinations. Treatment of $[PtCl_2(1,5-cod)]$ or $[PdCl_2(NCPh)_2]$ with a selection of the diphosphines (**3–5**) gave the expected chelate complexes, four of which, $[PtCl_2(\mathbf{3b})]$, $[PtCl_2(\mathbf{4a})]$, $[PtCl_2(\mathbf{4c})]$, and $[PdCl_2(\mathbf{4a})]$, have had their crystal structures determined.

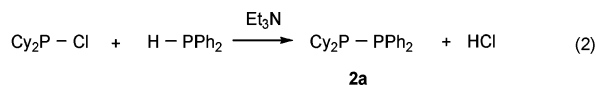
Introduction

Chelating diphosphines have been at the heart of organometallic chemistry and catalysis since the invention of dppe over 40 years ago.¹ The ready synthesis of chelating PCCP ligands having a 1,2-ethane backbone has led to the legion of variations on the structure with the substituents at P and C being used to control stereoelectronic effects (including chirality)² and solubility.³ Much less elaboration of diphosphines with 1,2-phenylene or 1,2-ethylene backbones has been reported despite the potential usefulness of backbone rigidity.⁴ Part of the reason for this is undoubtedly that the synthetic routes to diphos ligands with sp^2 -carbon backbones are not readily adaptable to the introduction of functionality. Here we report a general route to 1,2-ethylene diphosphines from readily accessible diphosphanes.

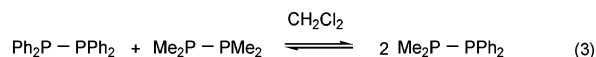
Diphosphanes have been known for over 100 years,⁵ but their applications in synthesis have been little explored.^{6,7} Tetraphenyldiphosphane **1a** is the most studied diphosphane and has been made by several methods^{8–10} from Ph_2PCl or Ph_2PH including catalytic dehydrogenative coupling of Ph_2PH .¹⁰ The route shown in eq 1 gave **1a** in 80% yield.⁸



Unsymmetrical diphosphanes have been made similarly; for example, **2a** was made¹¹ in 37% yield via the route shown in eq 2, although the product was contaminated with the symmetrical diphosphanes **1a** and P_2Cy_4 (**1b**).



Unsymmetrical diphosphanes are known to undergo metathesis reactions, e.g., the process shown in eq 3, which involves P–P bond cleavage.¹²



We report here the addition of P–P bonds across activated $C\equiv C$ bonds (diphosphination) as an efficient route to chelating diphosphinoethenes with ester-substituted backbones. Though P–P additions to alkynes have been previously reported,^{13,14} they are rare compared to the addition of other E–E bonds to alkynes.¹⁵

* Corresponding author. E-mail: paul.pringle@bristol.ac.uk.

[†] University of Bristol.

[§] Rhodia Inc.

(1) Aguiar, A. M.; Daigle D. *J. Am. Chem. Soc.* **1964**, *86*, 2299.

(2) For leading references see: (a) Wada, Y.; Imamoto, T.; Tsurutu, H.; Yamaguchi, K.; Gridnev, I. D. *Adv. Synth. Catal.* **2004**, *346*, 777. (b) Fries, G.; Wolf, J.; Ilg, K.; Walfort, B.; Stalk, D.; Werner, H. *Dalton Trans.* **2004**, 1873.

(3) (a) For, leading references see: Amrani, Y.; Lecomte; Sinou, D.; Bakos, J.; Toth, I.; Hell, B. *Organometallics* **1989**, *8*, 542. (b) Hanson, B. E. *Coord. Chem. Rev.* **1999**, *185–186*, 795. (c) Pinault, N.; Bruce, D. W. *Coord. Chem. Rev.* **2003**, *241*, 1.

(4) Freixa, Z.; van Leeuwen, P. W. N. M. *Dalton Trans.* **2003**, 1890, and references therein.

(5) Kosolopoff, G. M.; Maier L. In *Organic Phosphorus Compounds*; Wiley: New York, 1972; Vol. 1.

(6) Cowley, A. H. *Chem. Rev.* **1965**, *65*, 617.

(7) Caminade, A.-M.; Majoral, J.-P.; Mathieu, R. *Chem. Rev.* **1991**, *91*, 575.

(8) Kuchen, W.; Buchwald, H. *Chem. Ber.* **1959**, 227.

(9) (a) Spanier, E. J.; Caropreso, F. E. *Tetrahedron Lett.* **1969**, *3*, 199.

(b) Goldwhite, H.; Kaminski, J.; Millhauser, G.; Ortiz, J. E.; Bargas, M.; Vertal, L.; Lappert, M. F.; Smith, S. J. *Organometallic Chem.* **1986**, *310*, 21. (c) Calderazzo, F.; Pampaloni, G. *Polyhedron* **1998**, *7*, 2039. (d) Dick D. G.; Rousseau, R.; Stephan, D. W. *Can. J. Chem.* **1991**, *69*, 357.

(10) Böhm, V. P. W.; Brookhart, M. *Angew. Chem. Int. Ed.* **2001**, *40*, 4694.

(11) Issleib, K.; Krech, K. *Chem. Ber.* **1965**, *98*, 1093.

(12) (a) McFarlane, H. C. E.; McFarlane, W. J. *J. Chem. Soc., Chem. Commun.* **1972**, 1189. (b) Harris, R. K.; Norval, E. M. *J. Chem. Soc., Dalton Trans.* **1979**, 826.

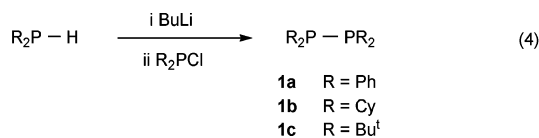
(13) Cullen, W. R.; Dawson, D. S. *Can. J. Chem.* **1967**, *45*, 2887.

(14) Sato, A.; Yorimitsu, H.; Oshima, K. *Angew. Chem. Int. Ed.* **2005**, *44*, 1694.

(15) Beletskaya, I.; Moberg, C. *Chem. Rev.* **2006**, *106*, 2320.

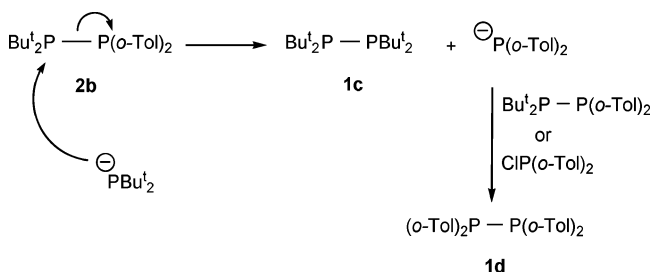
Results and Discussion

Diphosphane Synthesis. The symmetrical diphosphanes **1a–c** were made according to eq 4 and fully characterized (see Experimental Section).

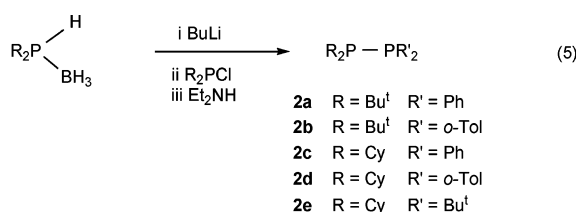


Attempts to extend this method to the synthesis of unsymmetrical diphosphanes **2a–e** gave the desired products in 40–75% yield (according to ³¹P NMR) but contaminated with significant amounts of symmetrical diphosphanes and other byproducts. For example, treatment of Bu^t₂PH with BuLi followed by (*o*-Tol)₂PCL gave a mixture of the desired Bu^t₂P–P(*o*-Tol)₂ **2b** (40%), the symmetrical diphosphanes **1c** (11%) and P₂(*o*-Tol)₄ (**1d**) (30%), Bu^t₂PH (16%), and Bu^t₂PCL (3%). We know from subsequent experiments (see below) that **2b** is stable to metathesis, and therefore **1c** and **1d** are likely formed by the comproportionation shown in Scheme 1.

Scheme 1. Comproportionation of Unsymmetrical Diphosphanes



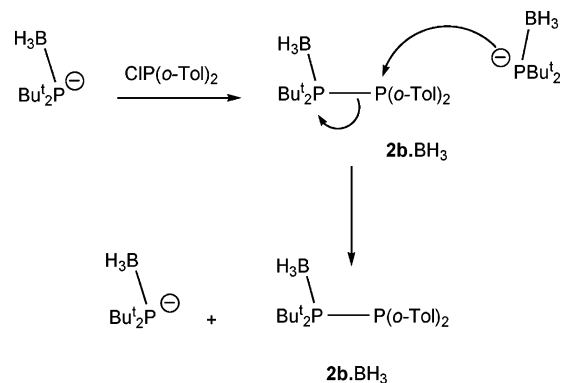
An efficient general route to pure unsymmetrical diphosphanes was found to be via the borane adducts of the secondary phosphines (eq 5). For example **2b** was formed almost exclusively (by ³¹P NMR), and when the product was stirred at ambient temperatures in THF for 72 h or refluxed in toluene for 1 h, there was no sign of metathesis to **1c** and **1d**.



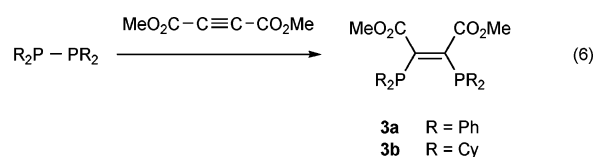
A mechanistic explanation for the high chemoselectivity of the reactions in eq 5 is given for **2b** in Scheme 2. In the intermediate diphosphane monoborane **2b**·BH₃, one of the P-centers is more crowded and therefore less susceptible to nucleophilic attack. Attack at the other phosphorus generates only the desired product.

Diphosphinations of Activated Alkynes. The symmetrical diphosphanes **1a** and **1b** were added to dimethylacetylene dicarboxylate (DMAD) in toluene at ambient temperatures. The reactions were followed by ³¹P NMR spectroscopy, which showed that the additions were rapid and gave the diphosphines **3a** and **3b** as the *cis* isomers exclusively (eq 6) (see Experimental Section for the characterizing data). The crystal structure of diphosphine **3b** has been determined (see below). The

Scheme 2. Borane-Assisted Synthesis of Unsymmetrical Diphosphanes

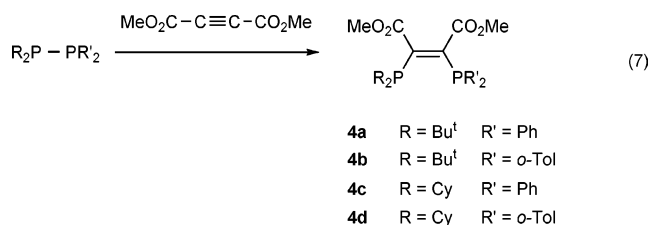


synthesis of diphosphine **3a** in three steps from 2,3-dichloromaleic acid anhydride has been previously reported.¹⁶

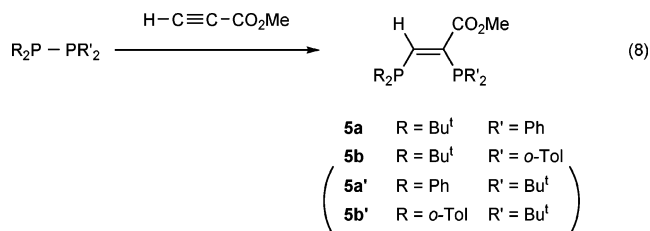


The very bulky diphosphane **1c** did not react with DMAD under ambient conditions or upon heating the reaction mixture for 3 days at 60 °C in the presence of the radical initiator AIBN.

The unsymmetrical diphosphanes **2a–d** all added smoothly to DMAD to give diphosphines **4a–d** according to eq 7 (see Experimental Section for the characterizing data).

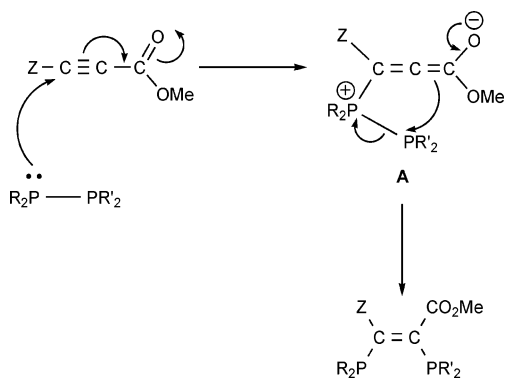


The symmetrical diphosphanes **1a** and **1b** did not react with the terminal acetylene methyl propiolate under the conditions in which they added rapidly to DMAD. However the unsymmetrical **2a** and **2b** did react with methyl propiolate to give **5a** and **5b** according to eq 8 (see Experimental Section for the characterizing data). Remarkably only one product was observed (i.e., the isomers **5a'** and **5b'** were not detected).



The proposed mechanism for the diphosphinations (eqs 6–8) is shown in Scheme 3. A contribution from a mechanism involving radicals cannot be ruled out but is considered unlikely because of the high *cis* stereoselectivity observed; radical-initiated P–P additions to terminal alkynes has recently been reported to give mainly *trans* alkenes.¹⁴

(16) Becher, H. J.; Bensmann, W.; Fenske, D.; Pfennig, B. *Monatsh. Chem.* **1978**, *109*, 1023, and references therein.

Scheme 3. Proposed Mechanism of Diphosphination of Activated Alkynes


Nucleophilic attack by the diphosphane on the Michael activated alkyne would give zwitterionic intermediate **A**. A zwitterionic intermediate has been proposed as an intermediate in the reaction of tertiary phosphines with DMAD to give phosphorus ylides.¹⁷ The intact P–P bond in **A** ensures that the subsequent intramolecular rearrangement gives the observed *cis* alkene product. The lability of the P–P bond in **A** is consistent with the propensity of cationic species of the type $R_2P-PR_3^+$ to undergo P–P cleavage reactions.⁶ The rate of the first step in Scheme 3 would depend on the electrophilicity of the alkyne, which explains the greater reactivity of DMAD than methyl propiolate. It would also depend on the nucleophilicity of the diphosphane, which explains why the nonpolar and very bulky **1c** is unreactive and why the isomer formed in the reaction of the unsymmetrical diphosphanes with methylpropiolate (eq 8) is derived from the attack of the more electron rich (PBu_2) end of the diphosphane. The rate of the reaction between **2b** and DMAD was faster at higher concentrations of DMAD and was faster in MeCN and CH_2Cl_2 than in toluene; these observations are consistent with the rate-limiting formation of the polar intermediate **A**.

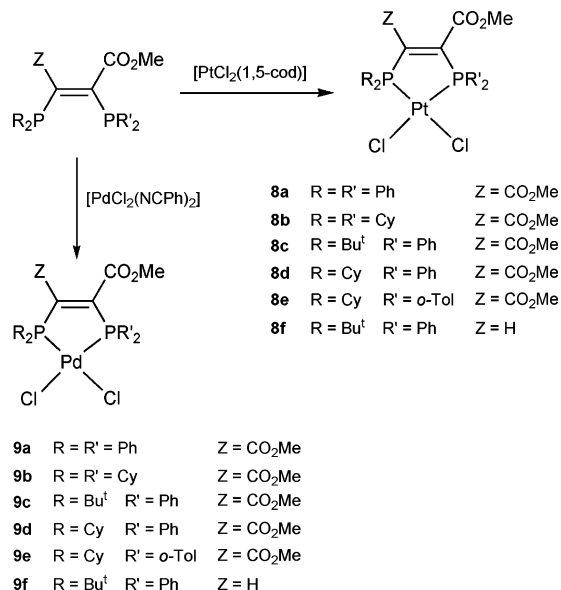
Platinum(II) and Palladium(II) Chelates. The coordination chemistry of none of the ligands discussed here has been previously reported.¹⁸ Treatment of $[PtCl_2(1,5-cod)]$ or $[PdCl_2(NCPh)_2]$ with diphosphinoethenes **3a,b**, **4a,c,d**, and **5a** in dichloromethane gave the expected chelates **8a–f** and **9a–f** (see Scheme 4).

The complexes were characterized by a combination of ³¹P, ¹H, and ¹³C NMR spectroscopy, IR spectroscopy, mass spectrometry, and X-ray crystallography. The ³¹P NMR spectra were particularly characteristic: the large coordination chemical shifts ($\Delta\delta$ 55–75 ppm for **8a–f** and 80–100 ppm for **9a–f**) are typical for five-membered chelates;¹⁹ the values of $\Delta\delta$ (e.g., $[PtCl_2(dppe)]$ 58.5 Hz, $[PdCl_2(dppe)]$ 81.5 Hz) and ¹J(PtP) (ca. 3500 Hz) are consistent with *cis* phosphines which are *trans* to Cl ligands. In addition, the crystal structures of the platinum complexes **8b**, **8c**, and **8d** and palladium complex **9c** have been determined.

(17) Tebby, J. C.; Wilson, I. F.; Griffiths, D. V. *J. Chem. Soc., Perkin Trans. 1* **1979**, 2133, and references therein.

(18) Complexes of the type $[MCl_2(Ph_2PCH=CRPR'_2)]$ (M = Pt, Pd; R = CF_3 , Ph, Bu^t; R' = Ph, CH_2CH_2CN) have been made by the reaction of PHR'_2 to $[MCl_2(Ph_2PC=CR)_2]$; see: Carty, A. J.; Johnson, D. K.; Jacobson, S. E. *J. Am. Chem. Soc.* **1979**, *101*, 5612. A platinum(II) complex of the maleic anhydride derivative $Ph_2PCH(CO)(O)=CH(CO)PPh_2$ has been described; see: Ravindar, V.; Schumann, H.; Hemling, H.; Blum, J. *Inorg. Chim. Acta* **1995**, *240*, 145. A dicobalt complex containing a bridging η^4 - $Me_2PCH(CO_2Me)=CH(CO_2Me)PMe_2$ ligand has also been reported; see: Zolk, R.; Werner, H. *J. Organomet. Chem.* **1987**, *331*, 95.

(19) Garrou, P. E. *Chem. Rev.* **1981**, *81*, 229.

Scheme 4. Platinum and Palladium Complexes of Diphosphinoethenes


X-ray Crystallography. Crystals of **3b** suitable for X-ray crystallography were obtained from a diethyl ether solution in the space group $P\bar{1}$ (see Figure 1 and Table 1 for selected bond lengths and angles). One of the cyclohexyl substituents on P2 was disordered over two positions with occupancies of about 74% and 26%. The structure was refined with a suitable restraint on the P–C bond length, and refinement proceeded smoothly to give the structure shown.

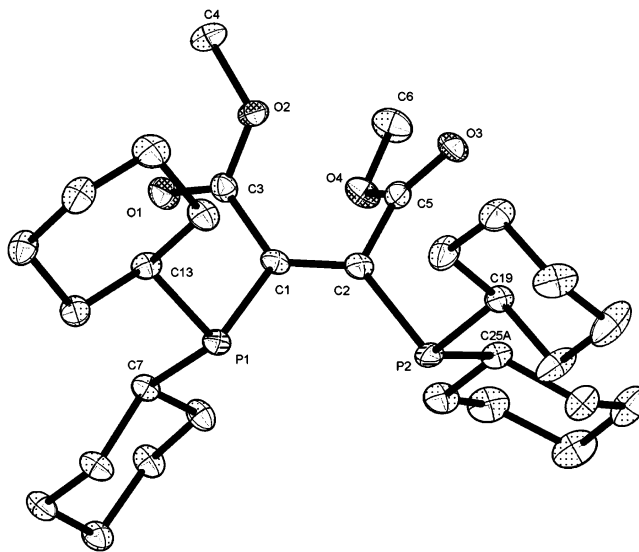


Figure 1. X-ray crystal structure of diphosphinoethene **3b**. Only the major component shown as the structure is disordered. Picture is shown with 50% ellipsoids. Hydrogen atoms are omitted for clarity.

Table 1. Selected Bond Lengths (Å) and Angles (deg) for Diphosphinoethene **3b**

P1–C1	1.8555(16)	C1–P1–C7	99.36(6)
P1–C13	1.8704(17)	C13–P1–C7	104.52(7)
P1–C7	1.8735(15)	C25B–P2–C2	113.2(3)
P2–C25B	1.817(4)	C25B–P2–C19	105.4(2)
P2–C2	1.8481(16)	C2–P2–C19	100.49(7)
P2–C19	1.8706(15)	C2–P2–C25A	94.99(10)
P2–C25A	1.915(2)	C19–P2–C25A	103.97(8)
C1–P1–C13	97.39(7)	P1–C1–C2–P2	1.98(18)

Crystals of **8b**, as a chloroform solvate, suitable for X-ray crystallography were obtained from a chloroform solution in the space group $P2_1/n$ (see Figure 2 and Table 2 for selected bond lengths and angles).

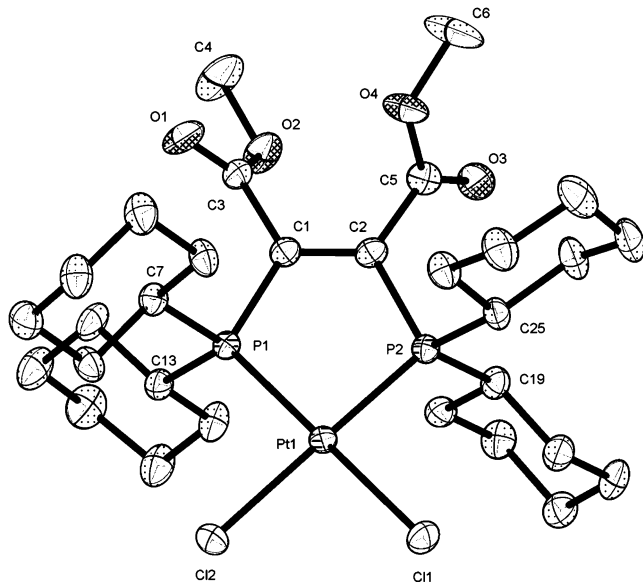


Figure 2. X-ray crystal structure of $[\text{PtCl}_2(\mathbf{3b})]$ (**8b**)· CHCl_3 . Picture is shown with 50% ellipsoids. Hydrogen atoms are omitted for clarity.

Table 2. Selected Bond Lengths (Å) and Angles (deg) for $[\text{PtCl}_2(\mathbf{3b})]$ (**8b**)· CHCl_3

Pt1–P1	2.2151(12)	P2–C19	1.855(5)
Pt1–P2	2.2182(12)	P1–Pt1–P2	89.04(4)
Pt1–Cl2	2.3568(12)	C1–P1–C13	107.7(2)
Pt1–Cl1	2.3581(12)	C1–P1–C7	103.2(2)
P1–C1	1.826(5)	C13–P1–C7	106.6(2)
P1–C13	1.830(5)	C25–P2–C2	106.9(2)
P1–C7	1.848(5)	C25–P2–C19	107.0(2)
P2–C25	1.839(5)	C2–P2–C19	103.7(2)
P2–C2	1.844(5)	P1–C1–C2–P2	2.1(5)

The orientation of the cyclohexyl groups may be described in terms of a quadrant diagram, where each of the cyclohexyl rings lies in a quadrant, with a torsion angle $\text{C}_{\text{backbone}}\text{--P--C}_{\text{cyclohexyl}}\text{--H}$ describing the rotation of the cyclohexyl around the P–C bond. Values ca. $\pm 60^\circ$ correspond to *gauche* conformations (g^+ or g^-) and values close to $\pm 180^\circ$ to *anti* (*a*). This is shown in Figure 3 for the free diphosphine (**3b**) and in Figure 4 for its complex **8b**. It is notable that in most cases (except the minor orientation of the disordered cyclohexyl in **3b**) diagonally opposite cyclohexyl groups adopt the same conformation.

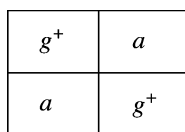


Figure 3. Quadrant diagram for **3b**.

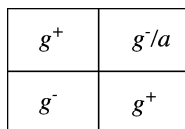


Figure 4. Quadrant diagram for **8b**.

Thus complexation of the ligand involves rotation of at least one of the cyclohexyl groups (that represented by the bottom

left quadrant). However, in other respects the diphosphine **3b** shows a high degree of preorganization for complexation to a metal; thus the phosphorus atoms are *syn* to each other, and the C1–C2–P2–C_{Cy} and C2–C1–P2–C_{Cy} torsions are such that the phosphorus lone pairs are ideally placed to chelate a metal, and even the CO₂Me groups on the backbone adopt a very similar conformation in the free phosphine and the complex. On complexation the P–C_{Cy} bond shortens (lengths in **3b**, 1.870(2)–1.874(2) and in **8b**, 1.826(5)–1.848(5)), although the change in the P–C_{backbone} bond lengths is not significant. There is a simultaneous increase in the CPC angles (ignoring parameters for disordered atoms).

Crystals of **8c**, as a chloroform solvate, suitable for X-ray crystallography were obtained from a chloroform solution in the space group $P\bar{1}$ (see Figure 5 and Table 3 for selected bond lengths and angles).

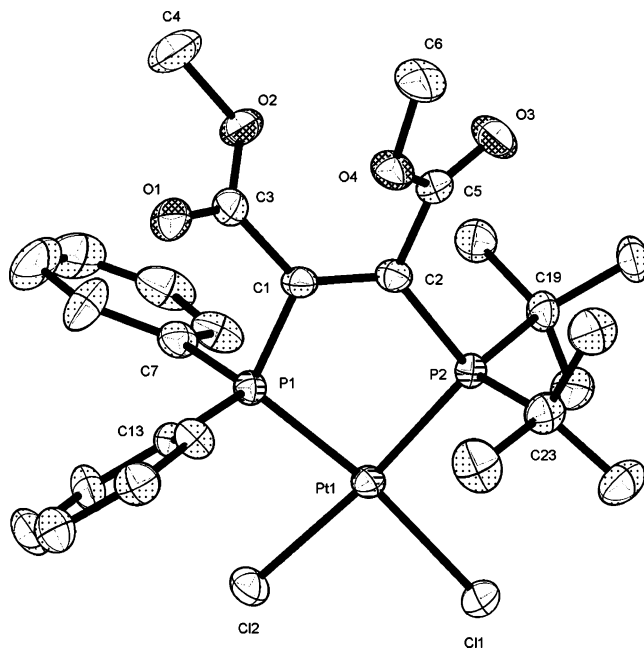


Figure 5. X-ray crystal structure of $[\text{PtCl}_2(\mathbf{4a})]$ (**8c**)· CHCl_3 . Picture is shown with 50% ellipsoids. Hydrogen atoms are omitted for clarity.

Table 3. Selected Bond Lengths (Å) and Angles (deg) for $[\text{PtCl}_2(\mathbf{4a})]$ (**8c**)· CHCl_3

Pt1–P1	2.1980(10)	P2–C19	1.895(4)
Pt1–P2	2.2654(11)	P1–Pt1–P2	88.70(4)
Pt1–Cl1	2.3549(11)	C13–P1–C7	107.7(2)
Pt1–Cl2	2.3743(10)	C13–P1–C1	104.89(19)
P1–C13	1.814(4)	C7–P1–C1	104.06(18)
P1–C7	1.817(4)	C2–P2–C23	104.44(19)
P1–C1	1.834(4)	C2–P2–C19	105.94(18)
P2–C2	1.865(4)	C23–P2–C19	113.6(2)
P2–C23	1.879(4)	P1–C1–C2–P2	2.5(5)

Crystals of **8d**, as a dichloromethane solvate, suitable for X-ray crystallography were obtained from a CH_2Cl_2 solution in the space group $P2_1/n$ (see Figure 6 and Table 4 for selected bond lengths and angles). The two cyclohexyl groups in **8d** mimic the g^+/a pattern of orientation seen in **8b**. In **8d**, there is no significant difference in the metal phosphorus bond lengths, despite the difference in substituents.

Crystals of **9c**, as a chloroform solvate, suitable for X-ray crystallography were obtained from a chloroform solution in the space group $P\bar{1}$ (see Figure 7 and Table 5 for selected bond lengths and angles).

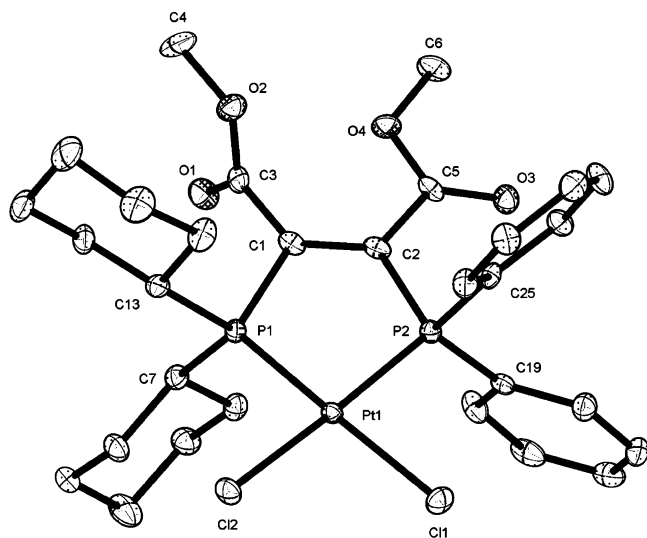


Figure 6. X-ray crystal structure of $[\text{PtCl}_2(\mathbf{4c})]$ ($\mathbf{8d}$) $\cdot\text{CH}_2\text{Cl}_2$. Picture is shown with 50% ellipsoids. Hydrogen atoms are omitted for clarity.

Table 4. Selected Bond Lengths (Å) and Angles (deg) for $[\text{PtCl}_2(\mathbf{4c})]$ ($\mathbf{8d}$) $\cdot\text{CH}_2\text{Cl}_2$

Pt1–P2	2.2074(15)	P2–C2	1.842(6)
Pt1–P1	2.2087(16)	P2–Pt1–P1	88.46(6)
Pt1–Cl1	2.3563(15)	C13–P1–C7	107.6(2)
Pt1–Cl2	2.3592(15)	C13–P1–C1	108.5(3)
P1–C13	1.835(5)	C7–P1–C1	101.5(3)
P1–C7	1.831(5)	C19–P2–C25	109.0(2)
P1–C1	1.846(6)	C19–P2–C2	107.1(3)
P2–C19	1.804(6)	C25–P2–C2	105.0(3)
P2–C25	1.819(5)	P1–C1–C2–P2	–10.4(6)

The crystal structures of $[\text{MCl}_2(\mathbf{4a})]\cdot\text{CHCl}_3$, $\mathbf{8c}$ ($\text{M} = \text{Pt}$) and $\mathbf{9c}$ ($\text{M} = \text{Pd}$), are isostructural. Both show distortion of coordination at the d^8 $\text{M}(\text{II})$ center from the square planar ideal; the chlorine (Cl1) *cis* to the phosphine with two *tert*-butyl groups (on P2) is positioned such that the angle P2–M–Cl1 is $98.17(4)^\circ$ for $\mathbf{8c}$ and $98.34(4)^\circ$ for $\mathbf{9c}$. The Cl1 is also displaced from the mean plane formed by M, P1, P2, and Cl2 by about 3° in each case.

The bond length M–P2 is longer than M–P1 in both $\mathbf{8c}$ and $\mathbf{9c}$, probably due to the steric requirements of the bulky *tert*-butyl substituents. Counterintuitively, the M–Cl2 bond *trans* to M–P2 is longer than the M–Cl1 by about 0.02 \AA . This implies that the higher *trans* influence of P1 than P2 (as indicated by the M–Cl bond lengths) is not reflected in their M–P bond lengths. The M–P1 bond length is comparable to the metal–phosphorus bond lengths in $\mathbf{8b}$ and $\mathbf{8d}$.

The five-membered $\text{MPC}=\text{CP}$ ring may also be characterized by a fold angle, i.e., the dihedral angle between the PMP and PCCP planes. In the crystal structures of the complexes reported here ($\mathbf{8b}$, $\mathbf{8c}$, $\mathbf{8d}$, and $\mathbf{9c}$) the $\text{MPC}=\text{CP}$ ring is effectively planar; none has a fold angle of more than 4° .

Finally, unlike *dppe* chelates, where the λ/δ ring conformations render the P-substituents inequivalent (pseudoaxial and pseudoequatorial), the rigid backbones in $\mathbf{8b–d}$ and $\mathbf{9c}$ make the P-substituents isoclinal.

Conclusion

Symmetrical and unsymmetrical diphosphanes have been shown to be readily accessible and show no evidence of metathesis under ambient conditions. The stereospecific and

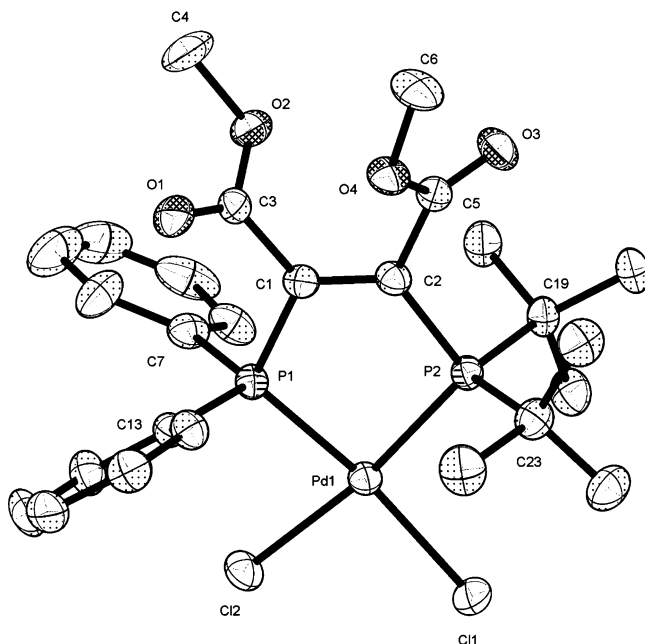


Figure 7. X-ray crystal structure of $[\text{PdCl}_2(\mathbf{4a})]$ ($\mathbf{9c}$) $\cdot\text{CHCl}_3$. Picture is shown with 50% ellipsoids. Hydrogen atoms are omitted for clarity.

Table 5. Selected Bond Lengths (Å) and Angles (deg) for $[\text{PdCl}_2(\mathbf{4a})]$ ($\mathbf{9c}$) $\cdot\text{CHCl}_3$

Pd1–P2	2.1933(9)	P2–C2	1.826(3)
Pd1–P1	2.2843(9)	P2–Pd1–P1	88.06(4)
Pd1–Cl2	2.3417(9)	C1–P1–C7	104.80(12)
Pd1–Cl1	2.3672(9)	C1–P1–C11	105.91(11)
P1–C1	1.855(3)	C7–P1–C11	113.62(12)
P1–C7	1.881(3)	C21–P2–C15	108.70(13)
P1–C11	1.887(3)	C21–P2–C2	104.42(12)
P2–C21	1.799(3)	C15–P2–C2	103.98(12)
P2–C15	1.806(3)	P1–C1–C2–P2	3.1(3)

regioselective diphosphination is a general method to a range of symmetrical and unsymmetrical chelating diphosphines featuring a rigid backbone bearing functional groups that should be amenable to further elaboration.

Experimental Section

Unless otherwise stated, all work was carried out under a dry nitrogen atmosphere, using standard Schlenk line techniques. Dry N_2 -saturated solvents were collected from a Grubbs system²⁰ in flame- and vacuum-dried glassware. NMR spectra were measured on a Jeol Eclipse 300 or a Jeol GX 400 spectrometer. Unless otherwise stated ^1H , ^{13}C , and ^{31}P NMR spectra were recorded at 400, 100, and 121 MHz, respectively at $+23^\circ\text{C}$. Mass spectra were recorded on a VG Analytical Autospec (EI) or VG Analytical Quattro (ESI). Elemental analyses were carried out by the Microanalytical Laboratory of the School of Chemistry, University of Bristol. $[\text{PtCl}_2(1,5\text{-cod})]^{21}$ and $[\text{PdCl}_2(\text{NCPH})_2]^{22}$ starting materials and (*o*-Tol) $_2\text{PCl}^{23}$ were made by literature methods, but all other phosphines were purchased from Strem. The compounds generally crystallized with chlorinated solvents (as shown by ^1H NMR

(20) Pangborn, A. B.; Giardello, M. A.; Grubbs, R. H.; Rosen, R. K.; Timmers, F. J. *Organometallics* **1996**, *15*, 1518.

(21) McDermott, J. X.; White, J. F.; Whitesides, G. M. *J. Am. Chem. Soc.* **1976**, *98*, 6521.

(22) Doyle, J. R.; Slade, P. E.; Jonassen, H. B. *Inorg. Synth.* **1960**, *6*, 218.

(23) Clark, P. W.; Mulraney, B. J. *J. Organomet. Chem.* **1981**, *217*, 51.

spectroscopy), which sometimes made elemental analyses for these compounds variable (see below).

1,1,2,2-Tetraphenyldiphosphane (1a).²⁴ To a solution of distilled Ph₂PH (0.93 cm³, 5.37 mmol) in THF (20 cm³) was added dropwise *n*-BuLi (1.6 M solution in hexanes, 4.4 cm³, 6.98 mmol) at -78 °C. After 30 min, the resulting solution was warmed to room temperature and stirred for 2 h. The solution was then cooled to -78 °C, Ph₂PCl (0.96 cm³, 5.37 mmol) was added, and the solution was stirred for 16 h. The solvent was removed under reduced pressure to leave the white solid product, which was then washed with methanol (2 × 20 cm³) and dried in vacuo to give **1a** as a white powder (1.62 g, 4.37 mmol, 81%). NMR data: ³¹P (CDCl₃) δ -14.6 (s); ¹H (300 MHz, CDCl₃) δ 7.45–7.32 (8H, m, CH), 7.32–7.14 (12H, m, CH); MS (ESI) *m/z* 371 (MH⁺); HRMS (ESI) calcd for C₂₄H₂₁P₂ 371.1124, found 371.1113.

1,1,2,2-Tetracyclohexyldiphosphane (1b).²⁵ **1b** was prepared from Cy₂PH and Cy₂PCl using the method described for **1a**, and recrystallization from methanol gave white crystalline solid **1b**, which was dried in vacuo (4.00 g, 10.14 mmol, 98%). NMR data: ³¹P (CDCl₃) δ -21.0 (s); ¹H (300 MHz, CDCl₃) δ 2.02–0.90 (44H, m, CH/CH₂); MS (ESI) *m/z* 411 ((M + O) H⁺); HRMS (ESI) calcd for the monoxide of **1b**, C₂₄H₄₅OP₂, 411.2947, found 411.2940.

1,1,2,2-Tetra-tert-butylidiphosphane (1c).²⁶ **1c** was prepared from Bu₂PH and Bu₂PCl using the method described for **1a**. Recrystallization from methanol gave white crystalline solid **1c**, which was dried in vacuo (0.30 g, 1.03 mmol, 30%). NMR data: ³¹P (CDCl₃) δ 40.6 (s); ¹H (300 MHz, CDCl₃) δ 1.31 (36H, t, J(PH) 6.2 Hz, CCH₃); ¹³C (CDCl₃) δ 34.8 (s, CCH₃), 33.0 (t, J(PC) 9 Hz, CCH₃); MS (ESI) *m/z* 291 (MH⁺); HRMS (ESI) calcd for C₁₆H₃₇P₂ 291.2376, found 291.2365.

1,1-Di-tert-butyl-2,2-diphenyldiphosphane (2a). To a solution of Bu₂PH·BH₃ (1.53 g, 9.55 mmol) (prepared from Bu₂PH and 1.1 equiv of BH₃·THF) in THF (20 cm³) was added dropwise *n*-BuLi (1.6 M solution in hexanes, 6.56 cm³, 10.50 mmol) at -78 °C. After 30 min, the solution was allowed to warm to room temperature, and the solution was then stirred for a further 2 h. The resulting solution was then added dropwise to a cooled (-78 °C) solution of Ph₂PCl (1.77 cm³, 2.11 g, 9.55 mmol) in THF (10 cm³), and then the mixture was allowed to warm to room temperature and stirred for 16 h. Et₃NH (4.93 cm³, 3.49 g, 47.73 mmol) was then added and the solution stirred for a further 16 h. The solvent was removed in vacuo, leaving an oily, white solid. Recrystallization from hot methanol (20 cm³) gave white solid **2a**, which was dried in vacuo (1.36 g, 4.13 mmol, 43%). NMR data: ³¹P (CDCl₃) δ 34.3 (d, ¹J(PP) 250 Hz, PBU₂), -25.7 (d, ¹J(PP) 250 Hz, PPh₂); ¹H (CDCl₃) δ 7.81 (4H, s, CH), 7.26 (6H, s, CH), 1.15 (18H, d, J(PH) 10.3 Hz, CCH₃); ¹³C (CDCl₃) with the aid of DEPT-135 δ 138.0 (dd, ¹J(PC) 20 Hz, ²J(PC) 6 Hz, *ipso*-C), 135.4 (dd, J(PC) 21 Hz, J(PC) 7 Hz, CH), 128.4 (s, CH), 128.1 (d, J(PC) 8 Hz, CH), 34.5 (dd, ¹J(PC) 28 Hz, ²J(PC) 8 Hz, CCH₃), 31.8 (dd, ²J(PC) 12 Hz, ³J(PC) 5 Hz, CCH₃); MS (ESI) *m/z* 347 ((M + O) H⁺); HRMS (ESI) calcd for the monoxide of **2a**, C₂₀H₂₉OP₂, 347.1698, found 347.1688.

1,1-Di-tert-butyl-2,2-di-*o*-tolylidiphosphane (2b). **2b** was prepared from Bu₂PH·BH₃ and (*o*-Tol)₂PCl using the method described for **2a**. Recrystallization from methanol gave white crystalline solid **2b**, which was dried in vacuo (5.24 g, 14.61 mmol, 91%). NMR data: ³¹P (CDCl₃) δ 32.4 (d, ¹J(PP) 203 Hz, PBU₂), -50.6 (d, ¹J(PP) 203 Hz, P(*o*-Tol)₂); ¹H (CDCl₃) δ 8.08–7.98 (2H, m, CH), 7.19–6.95 (6H, m, CH), 2.54 (6H, s, CCH₃), 1.12 (18H, d, ³J(PH) 10.6

Hz, CCH₃); ¹³C (CDCl₃) with the aid of DEPT-135 δ 142.5 (d, ¹J(PC) 29 Hz, *ipso*-C), 137.1 (d, J(PC) 15 Hz, CH), 130.0 (d, J(PC) 5 Hz, CH), 128.3 (s, CH), 125.4 (d, J(PC) 4 Hz, CH), 34.3 (dd, ¹J(PC) 29 Hz, ²J(PC) 10 Hz, CCH₃), 31.9 (dd, ²J(PC) 13 Hz, ³J(PC) 5 Hz, CCH₃), 21.7 (d, ³J(PC) 23 Hz, CCH₃); MS (ESI) *m/z* 375 ((M + O) H⁺); HRMS (ESI) calcd for the monoxide of **2b**, C₂₂H₃₃OP₂, 375.2009, found 375.2001.

1,1-Dicyclohexyl-2,2-diphenyldiphosphane (2c). **2c** was prepared from Cy₂PH·BH₃ and Ph₂PCl using the method described for **2a**. White solid **2c** was obtained from methanol and dried in vacuo (2.29 g, 6.00 mmol, 75%). NMR data: ³¹P (CDCl₃) δ -6.4 (d, ¹J(PP) 221 Hz, PCy₂), -28.2 (d, ¹J(PP) 221 Hz, PPh₂); ¹H (CDCl₃) δ 8.03–6.97 (10H, m, CH), 2.13–0.81 (22H, m, CH/CH₂); ¹³C (CDCl₃) with the aid of DEPT-135 δ 136.7 (dd, ¹J(PC) 20 Hz, ²J(PC) 7 Hz, *ipso*-C), 134.5 (dd, J(PC) 19 Hz, J(PC) 8 Hz, CH), 128.1 (m, CH), 32.9 (dd, J(PC) 20 Hz, J(PC) 9 Hz, CH), 32.0 (dd, J(PC) 12 Hz, J(PC) 8 Hz, CH₂), 31.0 (dd, J(PC) 10 Hz, J(PC) 6 Hz, CH₂), 27.4 (m, CH₂), 26.2 (m, CH₂); MS (ESI) *m/z* 399 ((M + O) H⁺); HRMS (ESI) calcd for the monoxide of **2c**, C₂₄H₃₃OP₂, 399.2009, found 399.2001.

1,1-Dicyclohexyl-2,2-di-*o*-tolylidiphosphane (2d). **2d** was prepared from Cy₂PH·BH₃ and (*o*-Tol)₂PCl using the method described for **2a**. Recrystallization from methanol gave white crystalline solid **2d**, which was dried in vacuo (2.42 g, 5.90 mmol, 84%). NMR data: ³¹P (CDCl₃) δ -6.2 (d, ¹J(PP) 197 Hz, PCy₂), -46.5 (d, ¹J(PP) 197 Hz, P(*o*-Tol)₂); ¹H (CDCl₃) δ 7.77–7.69 (2H, m, CH), 7.20–7.28 (6H, m, CH), 2.45 (6H, s, CCH₃), 1.82 (2H, d, CH, ²J(PH) 8.0 Hz), 1.74–1.54 (10H, m, CH₂), 1.32–1.03 (10H, m, CH₂); ¹³C (CDCl₃) with the aid of DEPT 135 δ 142.4 (dd, ²J(PC) 26 Hz, ³J(PC) 2 Hz, CCH₃), 136.1 (dd, ¹J(PC) 21 Hz, J(PC) 7 Hz, *ipso*-C), 135.0 (d, J(PC) 17 Hz, CH), 129.9 (d, J(PC) 5 Hz, CH), 128.2 (s, CH), 125.7 (s, CH), 33.3 (dd, J(PC) 20 Hz, J(PC) 11 Hz, CH), 32.6 (dd, J(PC) 15 Hz, J(PC) 8 Hz, CH₂), 31.8 (dd, J(PC) 10 Hz, J(PC) 5 Hz, CH₂), 27.8 (d, J(PC) 11 Hz, CH₂), 27.5 (d, J(PC) 9 Hz, CH₂), 26.3 (s, CH₂), 21.6 (d, ³J(PC) 21 Hz, CCH₃); MS (ESI) *m/z* 427 ((M + O) H⁺); HRMS (ESI) calcd for the monoxide **2d**, C₂₆H₃₇OP₂, 427.2323, found 427.2314.

1,1-Dicyclohexyl-2,2-di-tert-butylidiphosphane (2e). **2e** was prepared from Bu₂PH·BH₃ and Cy₂PCl using the method described for **2a**. Recrystallization from methanol gave white crystalline solid **2e**, which was dried in vacuo (0.96 g, 2.80 mmol, 65%). NMR data: ³¹P (CDCl₃) δ 22.9 (d, ¹J(PP) 395 Hz, PBU₂), -2.2 (d, ¹J(PP) 395 Hz, PCy₂); ¹H (CDCl₃) δ 2.10 (1H, s, CH), 1.95 (1H, s, CH), 1.89–1.56 (8H, m, CH₂), 1.47–1.11 (12H, m, CH₂), 1.26 (18H, d, J(PH) 11.72 Hz, CCH₃); ¹³C (CDCl₃) with the aid of DEPT 135 δ 34.7 (dd, J(PC) 5 Hz, ¹J(PC) 29 Hz, CCH₃), 33.9 (dd, J(PC) 7 Hz, J(PC) 14 Hz, CH₂), 32.5 (dd, ³J(PC) 5 Hz, ²J(PC) 13 Hz, CCH₃), 32.2 (dd, J(PC) 5 Hz, J(PC) 22 Hz, CH), 27.7 (d, J(PC) 11 Hz, CH₂), 26.4 (s, CH₂); MS (ESI) *m/z* 359 ((M + O) H⁺); HRMS (ESI) calcd for C₂₀H₄₁OP₂ 359.2643, found 359.2627.

(Z)-2,3-Bis(diphenylphosphino)but-2-enedioic Acid Dimethyl Ester (3a). To a solution of P₂Ph₄ (**1a**) (1.00 g, 2.70 mmol) in toluene (10 cm³) was added dimethylacetylene dicarboxylate (DMAD) (0.33 cm³, 0.38 g, 2.70 mmol), and this rapidly produced a deep red solution. ³¹P NMR indicated that the P–P bonded species had cleanly and selectively added to the alkyne. The solvent was removed under reduced pressure, and the resulting oil was dissolved in Et₂O. Yellow crystals of **3a** formed upon cooling the solution to -10 °C in a freezer, and these were filtered off, washed in Et₂O, and dried in vacuo to give a yellow crystalline powder of **3a** (0.50 g, 0.97 mmol, 36%). NMR data: ³¹P (CDCl₃) δ -11.9 (s); ¹H (CDCl₃) δ 7.38 (8H, m, CH), 7.26 (12H, m, CH) 3.22 (6H, s, CH₃); ¹³C (CDCl₃) with the aid of DEPT 135 δ 166.4 (m, C=O), 150.3 (s, C=C), 134.3 (t, J(PC) 2 Hz, *ipso*-C), 133.8 (t, J(PC) 11 Hz, CH), 129.0 (s, CH), 128.2 (t, J(PC) 4 Hz, CH), 51.6 (s, OCH₃); MS (ESI) *m/z* 513 (MH⁺); HRMS (ESI) calcd for C₃₀H₂₇O₄P₂ 513.1389, found 513.1379.

(24) Dashti-Mommertz, A.; Neumuller, B. *Z. Anorg. Allg. Chem.* **1999**, *625*, 954.

(25) Richter, R.; Kaiser, J.; Sieler, J.; Hartung, H.; Peter, C. *Acta Crystallogr.* **1977**, *B33*, 1887.

(26) (a) Aime, S.; Harris, R. K.; McVicker, E. M. *J. Chem. Soc., Chem. Commun.* **1974**, 251, 426. (b) Harlan, C. J.; Jones, R. A.; Koschmieder, S. U.; Nunn, C. M. *Polyhedron.* **1990**, *9*, 669.

(Z)-2,3-Bis(dicyclohexylphosphino)but-2-enedioic Acid Dimethyl Ester (3b). **3b** was prepared from P_2Cy_4 (**1b**) and DMAD using the method described for **3a**. Isolated, crystalline **3b** was obtained in only 16% yield, but **3b** can be generated quantitatively in situ (as shown by ^{31}P NMR) and used for further reactions. NMR data: ^{31}P ($CDCl_3$) δ -5.6 (s); 1H (300 MHz, $CDCl_3$) δ 3.72 (6H, s, CH_3), 1.94–1.56 (24H, m, CH/CH_2) 1.41–1.08 (20H, m, CH/CH_2); ^{13}C (75 MHz, $CDCl_3$) δ 168.4 (s, $C=O$), 153.2 (s, $C=C$), 52.0 (s, OCH_3), 36.0 (t, $J(PC)$ 6 Hz, CH_2), 30.9 (dt, $J(PC)$ 12 Hz, CH), 27.3 (dt, $J(PC)$ 21 Hz, CH_2), 26.4 (s, CH_2); MS (ESI) m/z 537 (MH^+); HRMS (ESI) calcd for $C_{30}H_{51}O_4P_2$ 537.3262, found 537.3257. Anal. (calc): C, 69.87 (67.14); H, 9.44 (9.39).

(Z)-2-(Di-tert-butylphosphino)-3-(diphenylphosphino)but-2-enedioic Acid Dimethyl Ester (4a). To a solution of $Bu^t_2P-PPh_2$ (**2a**) (0.10 g, 0.30 mmol) in toluene (5 cm^3) was added DMAD (0.04 g, 0.30 mmol), and this rapidly resulted in a deep red solution. ^{31}P NMR indicated that the P–P bonded species had cleanly and selectively added to the alkyne by the presence of one pair of doublets. The product **4a** thus generated was used in situ. NMR data: ^{31}P ($CDCl_3$) δ 30.4 (d, $^3J(PP)$ 182 Hz, PBu^t_2), -11.3 (d, $^3J(PP)$ 182 Hz, PPh_2).

(Z)-2-(Di-tert-butylphosphino)-3-(di-*o*-tolylphosphino)but-2-enedioic Acid Dimethyl Ester (4b). **4b** was prepared from $Bu^t_2P-P(o-Tol)_2$ (**2b**) and DMAD by the same method described for **4a** and used in situ. NMR data: ^{31}P ($CDCl_3$) δ 31.8 (d, $^3J(PP)$ 181 Hz, PBu^t_2), -27.1 (d, $^3J(PP)$ 181 Hz, $P(o-Tol)_2$).

(Z)-2-(Dicyclohexylphosphino)-3-(diphenylphosphino)but-2-enedioic Acid Dimethyl Ester (4c). **4c** was prepared from Cy_2P-PPh_2 (**2c**) and DMAD by the method described for **4a** and used in situ. NMR data: ^{31}P ($CDCl_3$) δ -3.7 (d, $^3J(PP)$ 167 Hz, PCy_2), -10.7 (d, $^3J(PP)$ 167 Hz, PPh_2).

(Z)-2-(Dicyclohexylphosphino)-3-(di-*o*-tolylphosphino)but-2-enedioic Acid Dimethyl Ester (4d). **4d** was prepared from $Cy_2P-P(o-Tol)_2$ (**2d**) and DMAD by the method described for **4a** and used in situ. NMR data: ^{31}P ($CDCl_3$) δ -2.7 (d, $^3J(PP)$ 172 Hz, PCy_2), -25.3 (d, $^3J(PP)$ 172 Hz, $P(o-Tol)_2$).

(Z)-3-(Di-tert-butylphosphino)-2-(diphenylphosphino)acrylic Acid Methyl Ester (5a). To a solution of $Bu^t_2P-PPh_2$ (**2a**) (0.308 g, 0.93 mmol) in toluene (5 cm^3) was added methyl propiolate (0.08 cm^3 , 0.078 g, 0.67 mmol), which resulted in a deep brown solution. ^{31}P NMR indicated that the P–P bonded species had cleanly and selectively added to the alkyne by the presence of two doublets. The product **5a** thus generated was used in situ. NMR data: ^{31}P ($CDCl_3$) δ 8.5 (d, $^3J(PP)$ 129 Hz, PBu^t_2), -11.6 (d, $^3J(PP)$ 129 Hz, PPh_2).

(Z)-3-(Di-tert-butylphosphino)-2-(di-*o*-tolylphosphino)acrylic Acid Methyl Ester (5b). **5b** was prepared from $Bu^t_2P-PTol_2$ (**2b**) and methyl propiolate by the method described for **5a** and used in situ. ^{31}P ($CDCl_3$) δ 9.3 (d, $^3J(PP)$ 124 Hz, PBu^t_2), -26.9 (d, $^3J(PP)$ 124 Hz, $PTol_2$).

[PtCl₂(3a)] (8a). A solution of ligand **3a** (0.10 g, 0.199 mmol) in CH_2Cl_2 (2 cm^3) was added dropwise to a solution of $[PtCl_2(1,5-cod)]$ (0.071 g, 0.119 mmol) in CH_2Cl_2 (6 cm^3). After 1 h the volume of the solution was reduced by half under vacuum. Et_2O (20 cm^3) was added dropwise, and **8a** precipitated out of solution as a white solid. The solid **8a** was filtered off, washed with Et_2O (3 \times 10 cm^3), and dried in vacuo (0.075 g, 0.096 mmol, 48%). NMR data: ^{31}P ($CDCl_3$) δ 49.5 (s, $^1J(PtP)$ 3637 Hz); MS (EI) m/z 778 (M^+), 743 ($M^+ - Cl$); IR $\nu(C=O)$ 1737 cm^{-1} .

[PtCl₂(3b)] (8b). A solution of ligand **3b** (0.035 g, 0.066 mmol) in CH_2Cl_2 (2 cm^3) was added dropwise to a solution of $[PtCl_2(1,5-cod)]$ (0.025 g, 0.067 mmol) in CH_2Cl_2 (2 cm^3). After 1 h the volume of the solution was reduced by half under vacuum. Et_2O (10 cm^3) was added dropwise, and **8b** precipitated out of solution as a white solid. The solid **8b** was filtered off, washed with Et_2O (3 \times 5 cm^3), and dried in vacuo (0.052 g, 0.065 mmol, 70%). NMR data: ^{31}P ($CDCl_3$) δ 68.4 (s, $^1J(PtP)$ 3587 Hz); 1H (300 MHz,

$CDCl_3$) δ 3.85 (s, 6H, CH_3), 1.98–1.58 (24H, m, CH/CH_2), 1.45–1.12 (20H, m, CH/CH_2); ^{13}C (75 MHz, $CDCl_3$) δ 164.5 (m, $C=O$), 151.6 (m, $C=C$), 53.5 (s, OCH_3), 35.2 (d, $J(PC)$ 31 Hz, CH_2), 31.1 (s, CH_2), 29.0 (m, CH), 27.1 (m, CH_2), 25.9 (s, CH_2); MS (EI) m/z 802 (M^+), 684 ($M^+ - 2 CO_2Me$); IR $\nu(C=O)$ 1736 cm^{-1} . Anal. (calc for **8b**·1/3 $CHCl_3$): C, 43.28 (43.25); H, 5.97 (6.02). This complex was also characterized by X-ray crystallography as a chloroform solvate.

[PtCl₂(4a)] (8c). **8c** was prepared from ligand **4a** and $[PtCl_2(1,5-cod)]$ using the method described for **8a**, giving an off-white solid (0.147 g, 0.168 mmol, 55%). NMR data: ^{31}P ($CDCl_3$) δ 97.9 (s, $^1J(PtP)$ 3704 Hz, PBu^t_2), 43.1 (s, $^1J(PtP)$ 3534 Hz, PPh_2); 1H ($CDCl_3$) δ 7.81 (4H, m, CH), 7.55 (2H, m, CH), 7.46 (4H, m, CH), 3.80 (3H, s, CH_3), 3.53 (3H, s, CH_3), 1.63 (18H, d, CH_3); ^{13}C ($CDCl_3$) δ 134.3 (d, $J(PC)$ 11 Hz, CH), 132.6 (s, CH), 128.7 (d, $J(PC)$ 12 Hz, CH), 125.6 (d, $^1J(PC)$ 70 Hz, *ipso-C*), 53.8 (s, OCH_3), 53.3 (s, OCH_3) 40.6 (d, $^1J(PC)$ 21 Hz, CCH_3), 30.4 (m, CCH_3); MS (EI) m/z 738 (M^+), 701 ($M^+ - Cl$), 644 ($M^+ - Cl - CO_2Me$), 608 ($M^+ - 2Cl - CO_2Me$); IR $\nu(C=O)$ 1744 cm^{-1} . Anal. (calc for **8c**· CH_2Cl_2): C, 38.58 (39.37); H, 3.80 (4.37).

[PtCl₂(4c)] (8d). **8d** was prepared from ligand **4c** and $[PtCl_2(1,5-cod)]$ using the method described for **8a**, giving a white solid (0.164 g, 0.207 mmol, 77%). NMR data: ^{31}P ($CDCl_3$) δ 71.3 (s, $^1J(PtP)$ 3544 Hz, PCy_2), 47.5 (s, $^1J(PtP)$ 3652 Hz, PPh_2); 1H ($CDCl_3$) δ 7.84–7.73 (4H, m, CH), 7.58–7.51 (2H, m, CH), 7.50–7.42 (4H, m, CH), 3.88 (3H, s, CH_3), 3.53 (3H, s, CH_3), 1.94–1.65 (12H, m, CH/CH_2), 1.45–1.17 (10H, m, CH/CH_2); ^{13}C ($CDCl_3$) δ 134.1 (d, $J(PC)$ 12 Hz, CH), 132.6 (s, CH), 128.7 (d, $J(PC)$ 12 Hz, CH), 125.7 (d, $^1J(PC)$ 68 Hz, *ipso-C*), 53.7 (s, OCH_3), 53.2 (s, OCH_3), 34.8 (d, $^1J(PC)$ 30 Hz, CH), 31.0 (s, CH_2), 28.4 (s, CH_2), 26.9 (dd, $J(PC)$ 8.5 Hz, $J(PC)$ 13 Hz), 25.9 (s); MS (ESI) m/z 813 (($M + Na$) H^+), 755 (($M - Cl$) H^+). Anal. (calc for **8d**·0.5 CH_2Cl_2) (calc): C, 43.68 (43.98); H, 4.94 (4.72). This complex was also characterized by X-ray crystallography as the dichloromethane solvate.

[PtCl₂(4d)] (8e). **8e** was prepared from ligand **4d** and $[PtCl_2(1,5-cod)]$ using the method described for **8a**, giving a white solid (0.077 g, 0.094 mmol, 40%). NMR data: ^{31}P ($CDCl_3$) δ 67.0 (s, $^1J(PtP)$ 3504 Hz, PCy_2), 44.3 (s, $^1J(PtP)$ 3721 Hz, $P(o-Tol)_2$); 1H ($CDCl_3$) δ 7.63 (1H, q, $J(HH)$ 7.7 Hz, CH), 7.52–7.38 (3H, m, CH), 7.34–7.16 (4H, m, CH), 3.86 (3H, s, OCH_3), 3.46 (3H, s, OCH_3), 2.67 (6H, d, $J(PH)$ 10.3 Hz, CCH_3), 2.22 (1H, s, CH), 2.11 (1H, s, CH), 1.96–0.90 (20H, m, CH_2); ^{13}C ($CDCl_3$) δ 143.4 (dd, $^4J(PC)$ 10 Hz, $^1J(PC)$ 40 Hz, *ipso-C*), 136.2 (d, $J(PC)$ 14 Hz, CH), 134.6 (d, $J(PC)$ 18 Hz, CH), 132.5 (t, $J(PC)$ 34 Hz, CH), 125.7 (t, $J(PC)$ 12 Hz, CH), 53.6 (s, OCH_3), 53.3 (s, OCH_3), 35.2 (d, $J(PC)$ 24 Hz, CH), 28.4 (m, CH_2), 26.8 (m, CH_2), 25.9 (d, $J(PC)$ 18 Hz, CH_2), 24.5 (d, $^3J(PC)$ 6 Hz, CCH_3), 23.5 (d, $^3J(PC)$ 6 Hz, CCH_3); MS (EI) m/z 781 ($M^+ - Cl$); IR $\nu(C=O)$ 1737 cm^{-1} . Anal. (calc for **8e**·0.5 CH_2Cl_2): C, 45.84 (45.33); H, 5.10 (5.03).

[PtCl₂(5a)] (8f). **8f** was prepared from ligand **5a** and $[PtCl_2(1,5-cod)]$ using the method described for **8a**, giving a gray solid (0.101 g, 0.149 mmol, 48%). NMR data: ^{31}P ($CDCl_3$) δ 70.0 (s, $^1J(PtP)$ 3619 Hz, PBu^t_2), 45.2 (s, $^1J(PtP)$ 3650 Hz, PPh_2); 1H ($CDCl_3$) δ 7.77 (4H, m, CH), 7.35 (6H, m, CH), 5.22 (1H, s, $C=CH$), 3.60 (3H, s, OCH_3), 1.47 (18H, dd, $J(HH)$ 2.3 Hz, $J(PH)$ 15.5 Hz, CCH_3); ^{13}C ($CDCl_3$) δ 161.3 (d, $J(PC)$ 23 Hz, $C=O$), 155.2 (dd, $J(PC)$ 25 Hz, $J(PC)$ 40 Hz, $C=C$) 134.5 (d, $J(PC)$ 12 Hz, CH), 132.2 (s, CH), 128.5 (d, $J(PC)$ 12 Hz, CH), 53.3 (s, OCH_3), 38.4 (d, $J(PC)$ 26 Hz, CCH_3), 30.4 (s, CCH_3); MS (EI) m/z 680 (M^+), 645 ($M^+ - Cl$); IR $\nu(C=O)$ 1727 cm^{-1} . Anal. (calc for **8f**· CH_2Cl_2): C, 38.42 (39.23); H, 4.40 (4.48).

[PdCl₂(3b)] (9b). A solution of ligand **3b** (0.054 g, 0.101 mmol) in CH_2Cl_2 (2 cm^3) was added dropwise to a solution of $[PdCl_2(NCPh)_2]$ (0.039 g, 0.101 mmol) in CH_2Cl_2 (2 cm^3). After 1 h the brown solution was reduced in volume by half and Et_2O (10 cm^3) added dropwise. The resulting pale orange solid **9b** was washed

Table 6. Crystal Data

	3b	8b ·CHCl ₃	8c ·CHCl ₃	8d ·CH ₂ Cl ₂	9c ·CHCl ₃
color, habit	yellow block	colorless block	colorless plate	colorless block	colorless block
size/mm	0.35 × 0.28 × 0.12	0.50 × 0.25 × 0.10	0.16 × 0.15 × 0.04	0.08 × 0.08 × 0.08	0.26 × 0.20 × 0.20
empirical formula	C ₃₀ H ₅₀ O ₄ P ₂	C ₃₁ H ₅₁ Cl ₅ O ₄ P ₂ Pt	C ₂₇ H ₃₅ Cl ₅ O ₄ P ₂ Pt	C ₃₁ H ₄₀ Cl ₄ O ₄ P ₂ Pt	C ₂₇ H ₃₅ Cl ₅ O ₄ P ₂ Pd
<i>M</i>	536.64	922	857.83	875.46	769.14
cryst syst	triclinic	monoclinic	triclinic	monoclinic	triclinic
space group	<i>P</i> 1	<i>P</i> 2 ₁ / <i>n</i>	<i>P</i> 1	<i>P</i> 2 ₁ / <i>n</i>	<i>P</i> 1
<i>a</i> /Å	11.359(2)	13.2422(10)	8.8712(5)	12.271(3)	8.844(3)
<i>b</i> /Å	11.784(2)	19.2312(19)	11.6350(7)	14.619(3)	11.587(5)
<i>c</i> /Å	12.843(3)	14.6945(11)	17.5707(10)	18.508(4)	17.470(7)
α/deg	100.44(3)	90	90.801(1)	90	90.783(9)
β/deg	94.37(3)	94.133(8)	104.334(1)	93.40(3)	104.471(8)
γ/deg	115.06(3)	90	108.685(1)	90	109.036(9)
<i>V</i> /Å ³	1508.7(7)	3732.4(5)	1655.89(17)	3314.3(12)	1637.8(11)
<i>Z</i>	2	4	2	4	2
μ/mm ⁻¹	0.176	4.236	4.768	4.688	1.108
<i>T</i>	100	173	173	100	173
no. of reflns: total/ indep/ <i>R</i> _{int}	17 343/6908/0.0223	24 867/6245/0.0560	17 698/7554/0.0572	22 940/7577/0.0618	17 320/7465/0.0316
final <i>R</i> ₁	0.0425	0.0320	0.0339	0.0378	0.0334
largest peak, hole/e Å ⁻³	0.615, -0.365	1.167, -1.084	2.643, -1.648	1.217, -1.239	1.147, -0.892

and dried in vacuo (0.048 g, 0.067 mmol, 72%). NMR data: ³¹P (CDCl₃) δ 95.8 (s); ¹H (CDCl₃) δ 3.85 (6H, s, CH₃), 2.22–1.02 (44H, m, CH/CH₂); ¹³C (75 MHz, CDCl₃) δ 164.4 (t, *J*(PC) 15 Hz, C=O), 151.0 (t, *J*(PC) 26 Hz, C=C), 53.7 (s, OCH₃), 36.2 (t, *J*(PC) 12 Hz, CH), 29.2 (d, *J*(PC) 17 Hz, CH₂), 27.1 (s, CH₂), 25.8 (s, CH₂); MS (EI) *m/z* 679 (M⁺ - Cl), 596 (M⁺ - 2 CO₂Me); IR ν(C=O) 1736 cm⁻¹.

[PdCl₂(**3a**)] (**9a**). **9a** as a pale orange solid (0.067 g, 0.097 mmol, 52%) was prepared in a fashion similar to **9b** from ligand **3a** and [PdCl₂(NCPPh₂)]. NMR data: ³¹P (CDCl₃) δ 71.8 (s); ¹H (300 MHz, CDCl₃) δ 7.93–7.84 (8H, m, CH), 7.67–7.59 (4H, m, CH), 7.57–7.49 (8H, m, CH), 3.56 (6H, s, CH₃); MS (ESI) *m/z* 713 (M + Na).

[PdCl₂(**4a**)] (**9c**). **9c** was prepared from ligand **4a** and [PdCl₂(NCPPh₂)] using the method described for **9b**, giving a pale orange solid (0.175 g, 0.269 mmol, 88%). NMR data: ³¹P NMR (CDCl₃) δ 126.6 (d, ²*J*(PP) 15 Hz, PBu₂), 65.0 (d, ²*J*(PP) 15 Hz, PPh₂); ¹H (CDCl₃) δ 7.77 (4H, dd, *J*(HH) 7.0 Hz, *J*(PH) 13.0 Hz, CH), 7.50 (2H, m, CH), 7.40 (4H, m, CH), 3.74 (3H, s, OCH₃), 3.45 (3H, s, OCH₃) 1.60 (18H, d, *J*(PH) 16.8 Hz, CH₃); ¹³C (CDCl₃) δ 165.6 (d, *J*(PC) 29 Hz, C=O), 163.1 (d, *J*(PC) 24 Hz, C=O), 153.6 (d, *J*(PC) 62 Hz, C=C), 152.0 (d, *J*(PC) 50 Hz, C=C), 134.4 (d, *J*(PC) 12 Hz, CH), 132.8 (d, *J*(PC) 3 Hz, CH), 128.8 (d, *J*(PC) 13 Hz, CH), 126.2 (d, *J*(PC) 54 Hz, *ipso*-C), 53.9 (s, OCH₃), 53.3 (s, OCH₃), 41.3 (d, *J*(PC) 12 Hz, CCH₃), 30.7 (d, *J*(PC) 4 Hz, CCH₃); MS (EI) *m/z* 615 (M⁺ - Cl), 599 (M⁺ - Cl - Me); IR ν(C=O) 1744 cm⁻¹. Anal. (calc for **9c**·1.5(CH₂Cl₂)): C, 42.69 (42.50); H, 4.83 (4.80). This complex was also characterized by X-ray crystallography.

[PdCl₂(**4c**)] (**9d**). **9d** was prepared from ligand **4c** and [PdCl₂(NCPPh₂)] using the method described for **9b**, giving a pale green solid (0.156 g, 0.223 mmol, 78%). NMR data: ³¹P (CDCl₃) δ 98.0 (d, ²*J*(PP) 19 Hz, PCy₂), 69.9 (d, ²*J*(PP) 19 Hz, PPh₂); ¹H (CDCl₃) δ 7.82 (4H, m, CH), 7.58 (2H, m, CH), 7.48 (4H, m, CH), 3.91 (3H, s, OCH₃), 3.55 (3H, s, OCH₃), 2.21 (2H, s, CH), 1.97–1.59 (12H, m, CH₂), 1.53–1.19 (8H, m, CH₂). ¹³C (CDCl₃) δ 134.2 (d, *J*(PC) 12 Hz, CH), 132.7 (d, *J*(PC) 3 Hz, CH), 128.9 (d, *J*(PC) 12 Hz, CH), 126.1 (d, *J*(PC) 59 Hz, *ipso*-C), 53.8 (s, OCH₃), 53.3 (s, OCH₃), 36.0 (d, *J*(PC) 22 Hz, CH), 28.8 (d, *J*(PC) 12 Hz, CH₂), 26.9 (d, *J*(PC) 13 Hz, CH₂), 25.7 (s, CH₂); MS (EI) *m/z* 665 (M⁺ - Cl), 584 (M⁺ - 2 CO₂Me); IR: ν(C=O) 1736 cm⁻¹. Anal. (calc for **9d**·1.5(CH₂Cl₂)): C, 45.36 (45.62); H, 5.27 (4.98).

[PdCl₂(**4d**)] (**9e**). **9e** was prepared from ligand **4d** and [PdCl₂(NCPPh₂)] using the method described for **9b**, giving a pale green solid (0.068 g, 0.093 mmol, 39%). NMR data: ³¹P (CDCl₃) δ 92.8 (d, ²*J*(PP) 17 Hz, PCy₂), 63.6 (d, ²*J*(PP) 17 Hz, P(*o*-Tol)₂); ¹H

(CDCl₃) δ 7.59–7.39 (4H, m, CH), 7.37–7.13 (4H, m, CH), 3.85 (3H, s, OCH₃), 3.43 (3H, s, OCH₃), 2.70 (6H, d, CCH₃, *J*(PH) 15.7 Hz), 2.29 (1H, s, CH), 2.08 (1H, s, CH), 1.91–1.47 (12H, m, CH₂), 1.42–1.03 (8H, m, CH₂); ¹³C NMR (CDCl₃) δ 164.9 (dd, *J*(PC) 3 Hz, *J*(PC) 30 Hz, C=O), 163.4 (dd, *J*(PC) 3 Hz, *J*(PC) 25 Hz, C=O), 154.1 (dd, *J*(PC) 28 Hz, *J*(PC) 35 Hz, C=C), 148.9 (dd, *J*(PC) 23 Hz, *J*(PC) 34 Hz, C=C), 143.6 (dd, *J*(PC) 11 Hz, *J*(PC) 60 Hz, CCH₃), 135.7 (d, *J*(PC) 13 Hz, CH), 134.4 (d, *J*(PC) 9 Hz, CH), 133.0 (s, CH), 132.6 (m, CH), 132.0 (d, *J*(PC) 9 Hz, CH), 125.9 (t, *J*(PC) 11 Hz, CH), 124.9 (dd, *J*(PC) 53 Hz, *J*(PC) 124 Hz, *ipso*-C), 53.6 (d, CCH₃, *J*(PC) 46 Hz), 36.8 (t, CH), 28.8 (dd, CH₂), 27.0 (m, CH₂), 25.8 (d, CH₂, *J*(PC) 19 Hz), 25.0 (d, CH₂, *J*(PC) 7 Hz), 23.8 (d, CH₂, *J*(PC) 9 Hz); MS (ESI) *m/z* 753 ((M + Na) H⁺), 695 ((M - Cl) H⁺). Anal. (calc for **9e**·2CH₂Cl₂): C, 45.69 (45.38); H, 5.07 (5.15).

[PdCl₂(**5a**)] (**9f**). **9f** was prepared from ligand **5a** and [PdCl₂(NCPPh₂)] using the method described for **9b**, giving a green solid (0.108 g, 0.183 mmol, 59%). NMR data: ³¹P (CDCl₃) δ 96.3 (d, ²*J*(PP) 21 Hz, PBu₂), 67.8 (d, ²*J*(PP) 21 Hz, PPh₂); ¹H (CDCl₃) δ 7.88 (4H, m, CH), 7.46 (6H, m, CH), 3.68 (3H, s, OCH₃), 1.58 (18H, d, *J*(PH) 15.7 Hz, CCH₃); ¹³C (CDCl₃) δ 154.6 (s, C=C) 134.5 (d, *J*(PC) 12 Hz, CH), 132.3 (d, *J*(PC) 2 Hz, CH), 128.6 (d, *J*(PC) 12 Hz, CH), 127.1 (d, *J*(PC) 60 Hz, *ipso*-C), 53.4 (s, OCH₃), 39.5 (d, *J*(PC) 18 Hz, CCH₃), 30.3 (d, *J*(PC) 4 Hz, CCH₃); MS (EI) *m/z* 557 (M⁺ - Cl); IR ν(C=O) 1728 cm⁻¹. Analysis (calc for **9f**·2CH₂Cl₂): C, 41.89 (41.00); H, 3.87 (4.73).

Crystal Structure Determinations. X-ray diffraction experiments on **8d** (as its dichloromethane solvate) and **3b** were carried out at 100 K on a Bruker SMART APEX diffractometer; experiments on **8b**, **8c**, and **9c** (all three as their chloroform solvates) were carried out at 173 K on a Bruker SMART diffractometer, using Mo Kα X-radiation (λ = 0.71073 Å). All data collections were performed using a CCD area detector, from a single crystal coated in paraffin oil mounted on a glass fiber. Intensities were integrated from several series of exposures, each exposure covering 0.3° in ω. Absorption corrections were based on equivalent reflections using SADABS V2.10,²⁷ and structures were refined against all *F*_o² data with hydrogen atoms riding in calculated positions using SHELXTL.²⁸ Crystal and refinement data are given in Table 6.

Except for **3b** (described earlier), no disorder was present in the other crystal structures, and refinements proceeded smoothly to give the structures shown.

(27) Sheldrick, G. M. *SADABS*, Bruker-Nonius area detector scaling and absorption correction (V2.10); University of Goettingen: Germany, 2003.
(28) *Shelxtl* Version 6.14; Bruker AXS, 2000–2003.

Acknowledgment. We thank Gordon Docherty (Rhodia) for useful discussions, Rhodia for a studentship (to D.L.D.), EPSRC for financial support, Johnson Matthey for a loan of precious metal compounds, and The Leverhulme Trust for a Research Fellowship (to P.G.P.).

Supporting Information Available: X-ray crystal data in CIF format for complexes **3b**, **8b**, **8c**, **8d**, and **9c** are available free of charge via the Internet at <http://pubs.acs.org>.

OM060716O